INVESTIGATION OF THE PROPERTIES OF OPTICAL FIBERS (IN THE UV SPECTRAL REGION) AND OPTOELECTRONIC COMPONENTS OPERATING IN RADIATION FIELDS OF FUSION INSTALLATIONS

D. Sporea, Adelina Sporea*, Mihaela Gherendi*, C. Oproiu* and B. Constantinescu***
**National Institute for Lasers, Plasma and Radiation Physics, Magurele*
*** National Institute of R&D for Physics and Nuclear Engineering – "Horia Hulubei", Magurele*

Subtask objectives

As semiconductor laser technology and material research advance, it is expected that such devices will play a major role in remote sensing and diagnostics systems, eye-in-hand robotic sub-assemblies, non-destructive measurements (interferometry, vibrometry, spectroscopy, etc.), optical communications. All these operations are of interest for remote handling tasks and control in fusion installations (i.e. ITER, DEMO). Their use under irradiation conditions (gamma, neutron) is a real challenge, hence the interest on the study of these devices behavior as they are subjected to irradiation.

Our research subject within the subtask is to evaluate:

- the modifications induced by the radiation existing in fusion installations in some optoelectronic semiconductor components, such as semiconductor lasers and detectors,

- the changes produced by irradiation and temperature on the optical transmission, in the UV and visible spectral ranges, in optical fibers used for plasma diagnostics.

1. Radiation induced modifications on semiconductor lasers used in the visible range and in optical fiber communications links

Concerning the semiconductor laser diodes investigations we followed several directions:

a) to extend the total irradiation doses range (both gamma-ray and electron beam irradiation) to which the devices were subjected;
b) to diversify the range of the investigated parameters (the temporal behavior of the emitted optical power and emitted radiation wavelength, the spectral characteristics of each laser diode upon each irradiation, and the temporal change of the laser diodes longitudinal mode structures);
c) to further develop the Laboratory capabilities, in order to acquire and to process more accurately high amounts of experimental data.

1.1 Data acquisition and processing

Until the reporting date of the last year report (December 2002), laser diodes operation driving current and case temperature were set manually, from the front panel of the diode driver/ temperature controller. In order to improve the accuracy of our investigation and to increase the speed of the data collection, we developed, in the frame of the National Instruments LabVIEW graphical programming environment, some special programmes designed to synchronously control various apparata and to assemble, in an appropriate manner, the results of the measurements. The programmes suite makes possible a programmatical stepping of the driving current of the laser diode under test, for different case temperatures. The driving current and the case temperature lower and upper limits are automatically set by the appropriate VI's, as soon as the operator selects the laser diode type to be measured. During the data collection the following linked parameters are saved together: the driving current; the laser diode case temperature; its compliance voltage; the wavelength of the emitted optical signal; the level of the emitted optical power; the instant value of the laser diode embedded photodiode current. The results are automatically saved in Excel compatible files on the controlling PC hard disk. From these files data are processed in order to: represent graphically the dependency of various characteristics on the temperature and total irradiation dose; to compute significant parameters for the laser diode, such as: the serial resistance, the external quantum efficiency, the threshold current, the photodiode responsivity.

1.2 New results on laser diodes irradiation

During the reporting period, we continue our investigation on radiation effects on semiconductor laser diodes (SLD) we started in 2002. The irradiation conditions (geometry, temperature) were identical with those already described in our Annual Report for 2001 [1]. The irradiation doses were increased for gamma-ray from 30 Mrad to 96 Mrad (in total dose steps: 34 Mrad, 44 Mrad, 60 Mrad, 76 Mrad and 96 Mrad), and for electron beam from 16 Mrad to 88 Mrad (in total dose steps: 21 Mard,
26 Mrad, 32 Mrad, 44 Mrad, 56 Mrad, 72 Mrad, 80 Mrad and 88 Mrad).

A. Terminology, notations, and measurement accuracy

To improve the accuracy of our measurements, we paid more attention to the evaluation of the uncertainties involved in the processing of the obtained data, as far as data acquisition errors can be neglected, as there is no involvement form the operator part. [2] In order to emphasis the changes induced by the irradiation process we have to determine as accurate as possible the value of some parameters, namely: the threshold current, the external quantum efficiency, the photodiode responsivity and the serial resistance of the laser diode. As it is quite difficult to locate the threshold current, we performed ***all*** data acquisition both at the increase and the decrease of the driving current.

The efficiency of the device (the ratio of the emitted optical power to its driving current) is specified by the ***external quantum efficiency*** (or differential efficiency) - η.

The next parameter of interest for the characterization of a laser diode is its (static***) serial resistance*** (Rs). The serial resistance represents the slope of the V(I) curve. It is defined for the values of the driving current above the threshold current value.

To evaluate the errors induced by the measuring process, we plotted also the error existing between the direct voltage vs. driving current curves when the current through the laser diode increases and decreases. It proves that over the measuring range these errors are extremely small (less than 0.05 %).

The determination of the ***wavelength*** of the emitted optical radiation implies by its-self some errors due to the measuring principle involved (in our case, the use of dual spectral responsivity detectors). Besides this aspect, some errors are also produced by the multimode structure of the emitted spectra. For this reason, we performed data collection both when the driving current is increased and when it is decreased.

B. Results

Some examples of the results obtained are given bellow, both for gamma-ray and electron beam irradiation. For data processing we used the data computing and visualization software "Origin".

Optical characteristics

The effects of electron-beam irradiation on quantum well lasers optical power is illustrated in Figure 1 a for the laser diode SLD3, where we plotted this parameter dependence on the laser driving current and case temperature. Similar curves are available for the other diodes, too. Similar data are available for gamma irradiation (Figure 1 b). We represented only the extreme case temperature values used for each laser, as well as the minimum and the maximum total irradiation doses related to this experimental investigation.

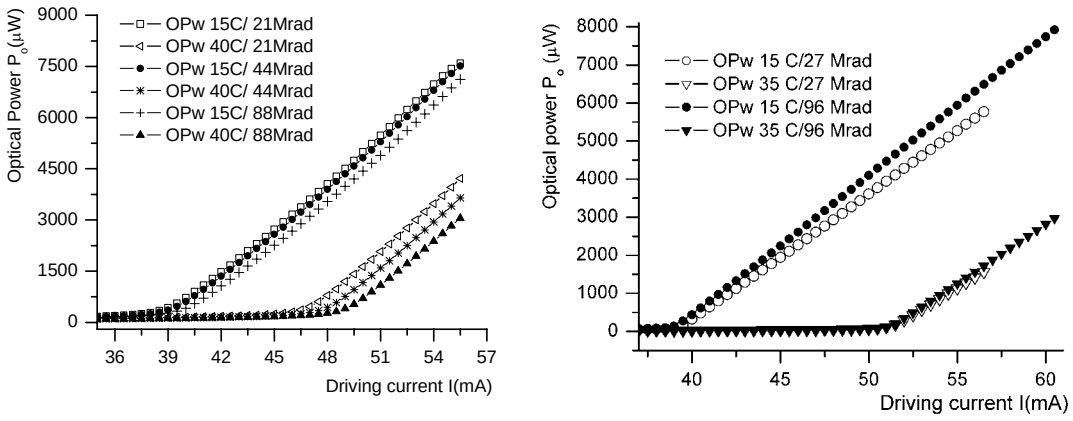

a b

Figure 1. The optical power (P_o) vs. the laser driving current (I), as function of the total irradiation dose and the case temperature, for SLD3 irradiated by an electron beam (a) and gamma-ray (b).

In Figures 2 a and 2 b the change of the threshold current and the external quantum efficiency with the case temperature and the total irradiation dose is given, as an example. As can be observed from these curves, the change of the threshold current with the total irradiation dose is quite small as compared to the influence of the case temperature over the same parameter. On the other hand, the laser operation is affected by the irradiation as its external quantum efficiency (differential efficiency) is modified.

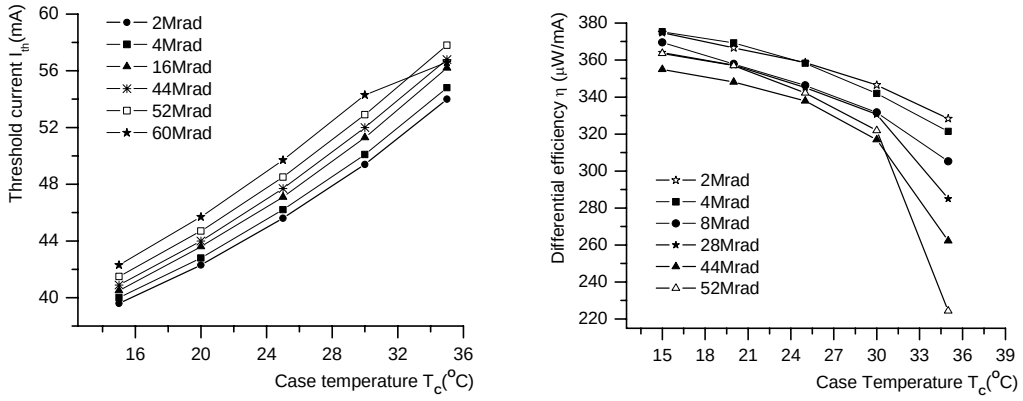

a b

Figure 2. The change of the laser threshold current (I_{th}) (a) and external quantum efficiency (b), as a function of the case temperature (T_c) and the total irradiation dose, for SLD1 (electron beam irradiation).

Another parameter investigated was the embedded photodiode responsivity (Figure 3).

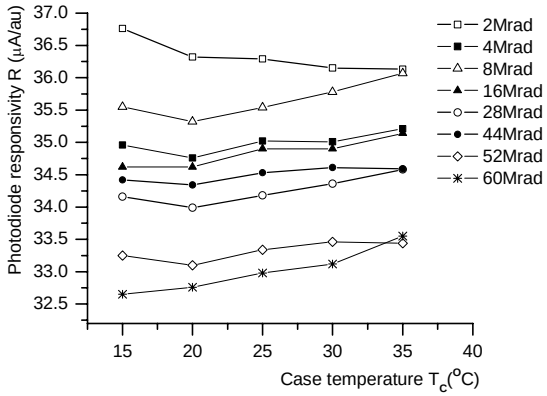

Figure 3. The change of the monitoring photodiode responsivity (R) as a function of the case temperature (T_c) and the total irradiation dose, for SLD1 (electron beam irradiation).

Electrical characteristics

In Figure 4 is represented, as an example, the modification of the laser direct voltage (compliance voltage) vs. the driving current, as the total irradiation dose change, for the laser diode SLD1 (electron beam irradiation), at the case temperature of 15 ^{O}C. Curves for other lasers are similar. From these characteristics we deduced the laser serial resistance (the slope of the voltage vs. driving current curve in its linear part) and the voltage corresponding to the threshold current (Figure 5).

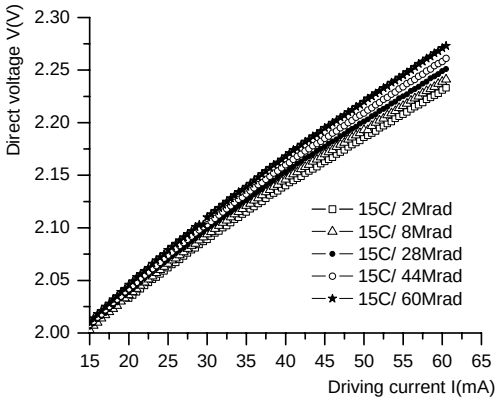

Figure 4. The compliance voltage (V) vs. the driving current (I), as a function of the total irradiation dose, for the case temperature of 15 ^{O}C, for SLD1 (electron beam irradiation).

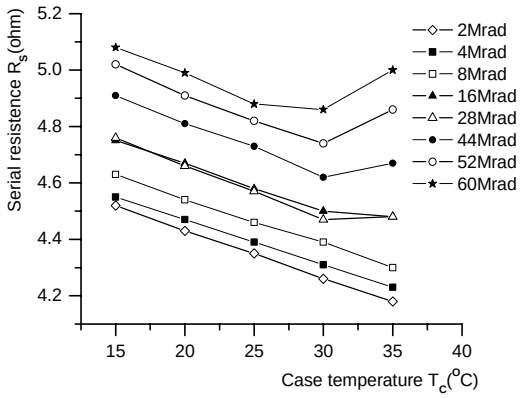

Figure 5. The change of the laser serial resistance (Rs) as a function of the case temperature (T_c) and the total irradiation dose, for SLD1 (electron beam irradiation).

Spectral characteristics

As an example, in Figure 6 is reproduced the change of the emitted wavelength, with the driving current and the total irradiation dose for SLD2 (electron beam irradiation), above the threshold point, at a case temperature of 15 ^{O}C. Similar curves were derived for all the laser diodes, for various total irradiation doses.

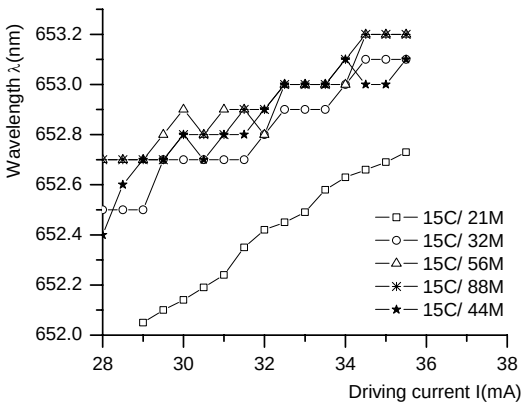

Figure 6. The change of laser wavelength (λ) asa function of the driving current (I) and the total irradiation dose, at a case temperature of 15 ^{O}C, for SLD2 (electron beam irradiation).

Figures 7 a and b depicts the influence of the total radiation dose (electron beam irradiation) over the spectrum of the emitted laser beam. A slight broadening of the full-width-half-maximum (FWHM) can be noticed as the total irradiation dose increases from 44 Mrad to 88 Mrad (SLD2).

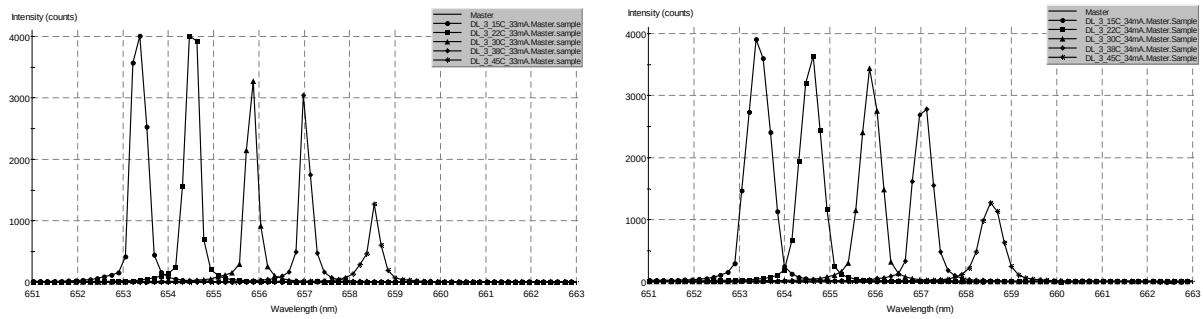

a b

Figure 7. The influence of the total irradiation dose on the emitted spectrum bandwidth (SLD2.), for the driving conditions, from left to right: dot – 15 ^{0}C/ 34 mA; rectangle – 22 ^{0}C/ 34 mA; triangle – 30 ^{0}C/ 34 mA; diamond – 38 ^{0}C/ 34 mA; star – 45 ^{0}C/ 34 mA, and the total irradiation dose of 44 Mrad (a) and 88 Mrad (b).

For the diode lasers studied, the following changes were observed (depending on the laser type and its operating conditions): [3]

- an increase of the threshold current up to 2 % for gamma irradiation and up to 7 % electron irradiation;
- a change of the differential efficiency up to 11 % for gamma irradiation and up to 6 % for electron irradiation;
- a decrease of the embedded photodiode responsivity (about 11 % for both types of irradiation);
- the serial resistance for all lasers increases (by 12 % for gamma irradiation and by 11 % for electron);
- the emitted radiation wavelength exhibits a blue shift of 0.3 nm for some lasers, or a red shift for others (up to 4 nm);
- the spectrum of the laser radiation broadens upon irradiation (typical situations: 1 - 2 nm, measured as the value of the half-peak bandwidth);
- no significant changes can be observed in the emitted radiation transversal beam structure.

The next step in our research on semiconductor lasers will be directed towards a comparative study of gamma-ray, neutron and electron beam irradiation on such optical radiation emitters.

2. Combined UV-exposure and Gamma radiation induced degradation in optical fibers to be used for diagnostics in fusion installations

As it concerns the optical fiber problem we concentrated on:

a) the diversification of irradiation sources used (we introduced also UV exposure of optical fibers);
b) the improvement of the measuring accuracy of the radiation induced optical absorption.

For the remote diagnostics of plasma, adequate connection links to transfer the measuring signal in media with high electromagnetic disturbances are needed. Optical channels have to be employed for electromagnetic immunity. Reported data on such investigation were carried out mostly in the visible and IR regions (400 nm and higher), considering the optical fiber as data transfer links or image guides. Very few data are available on the ionizing radiation degradation of the UV transmission of optical fibers. As is expected for these optical fibers to be employed to pick up the UV radiation from the investigated plasma, an additional decrease of the optical transmission can appear because of the UV induced increased absorption. [4]

The purpose of our investigation at this stage was to assess the effects of various external factors on the optical transmission. We used a 400 μm core diameter, enhanced UV transmission optical fiber, resistant to a temperature of 140 ^{O}C. The investigated optical fiber was cut in 24 cm long samples which were subjected to different treatments:

- gamma irradiation and temperature cycling;
- UV exposure and temperature cycling;
- UV, gamma and temperature cycling.

The maximum length of the optical fiber samples is imposed by the irradiation geometry.

The UV exposure was done with a stabilized CW operation, continuum spectrum deuterium lamp, (maximum fluctuation of 0.05 % p-p, and a drift of +/- 0.5 %/h), which was also used for the measurement of the spectral absorption of the optical fiber. For this purpose, a temporal SMA connector was attached to the fiber for a direct coupling to the source output.

- Gamma irradiations were done at the *Department of Applied Nuclear Physics* facility of "Horia Hulubei" National Institute of R&D for Physics and Nuclear Engineering, in Bucharest. The irradiation geometry was presented in detail in our 2002 report. Gamma irradiation was applied in 250 krad steps. All the measurements were carried out off-line, before and after each treatment, at the *Laser Metrology and Standardization Laboratory* facility, with the set-up based on a multi-channel optical fiber spectrometer, described in the 2002 report.

Significant results are presented in the Figures below.

Case 1.

An UV enhanced transmission optical fiber subjected to successive gamma irradiation and temperature stress.

Legend to Figure 8:

red – non-irradiated optical fiber; **blue** – gamma irradiation at 250 krad; **magenta** - gamma irradiation at 250 krad, followed by a temperature stress at 140 ^{O}C, for 2 h; **green** – gamma irradiation at 250 krad, followed by a temperature stress at 140 ^{O}C, for 2 h, and a new gamma irradiation at 250 krad; **cyan** – gamma irradiation at 250 krad, followed by a temperature stress at 140 ^{O}C, for 2 h, another gamma irradiation at 250 krad, and a final temperature stress at 140 ^{O}C, for 4 h.

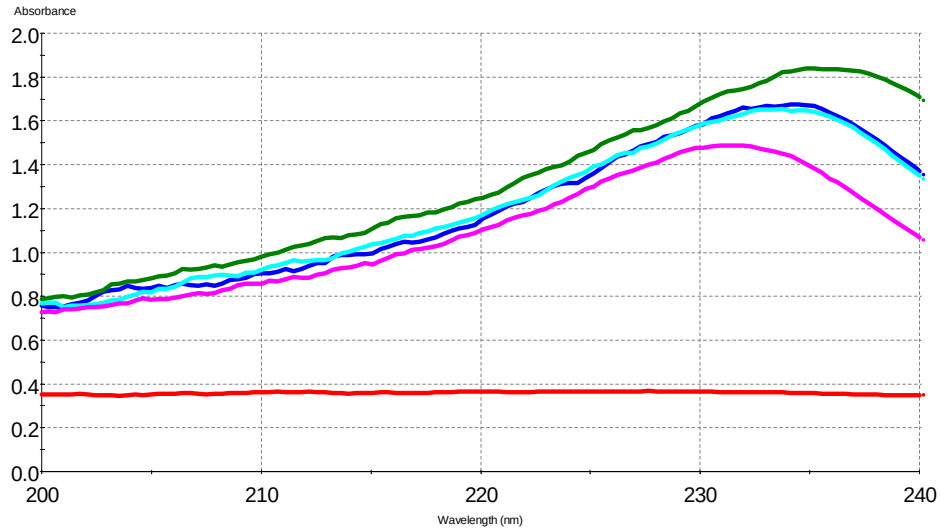

Figure 8. The spectral interval 200 nm – 240 nm.

Case 2.

An UV enhanced optical fiber was subjected to alternating UV exposure and temperature stress.

Legend to Figure 9:

red - non-irradiated optical fiber; **blue** – exposure to UV for 2 h; **light green** – exposure to UV radiation in two steps (2 h and 4 h); **magenta** – exposure to UV radiation in three subsequent steps (2 h, 4 h and 4 h); **brown** – exposure to UV radiation in three steps (2 h, 4 h and 4 h) followed by temperature stress at 50 ^{O}C for 1 h; **cyan** - exposure to UV radiation in three steps (2 h, 4 h and 4 h) followed by temperature stress at 50 ^{O}C (for 1 h) and at 100 ^{O}C (for 2 h); **dark green** – exposure to UV radiation in three steps (2 h, 4 h and 4 h) followed by temperature stress at 50 ^{O}C (for 1 h), at 100 ^{O}C (for 2 h), and another exposure to UV radiation for 4 h; **violet**: exposure to UV radiation in three steps (2 h, 4 h and 4 h), followed by temperature stress at 50 ^{O}C (for 1 h) and at 100 ^{O}C(for 2 h), and another exposure to UV radiation for 4 h, followed by a temperature stress at 140 ^{O}C (for 2 h).

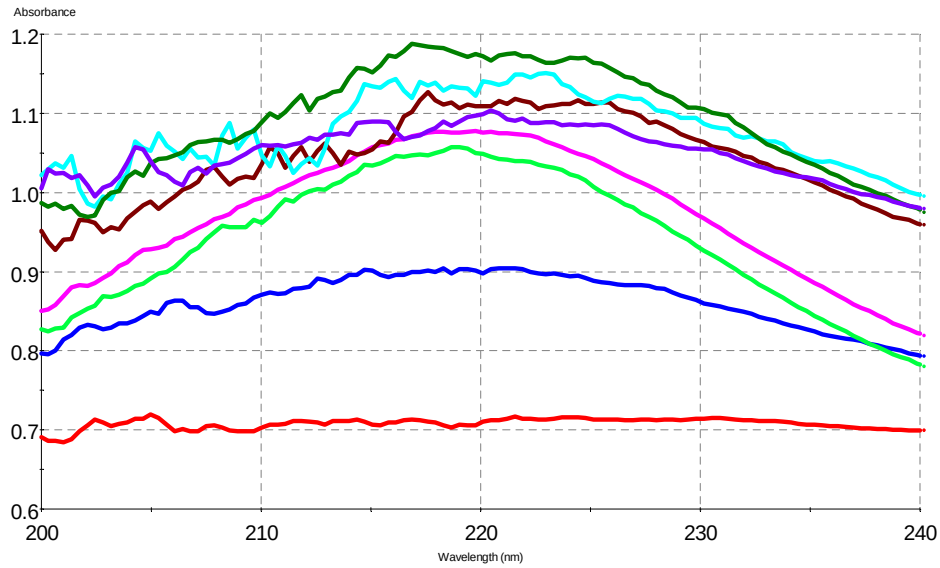

Figure 9. The spectral interval 200 nm – 240 nm.

Case 3.

An UV enhanced optical fiber was subjected to alternating UV exposure, gamma irradiation and temperature stress.

Legend to Figures 10:

red - non-irradiated optical fiber; **blue** – exposure to UV for 2 h; **light green** – exposure to UV radiation for 2 h, followed by gamma irradiation at the dose of 250 krad; **magenta** – exposure to UV radiation for 2 h, followed by gamma irradiation at the dose of 250 krad, and a temperature stress at 140 ^{O}C for 2 h; **brown** – exposure to UV radiation for 2 h, followed by a gamma irradiation at the dose of 250 krad, a temperature stress at 140 ^{O}C for 2 h, and a final exposure to UV radiation for 2 h; **cyan** – exposure to UV radiation for 2 h, followed by a gamma irradiation at the dose of 250 krad, a temperature stress at 140 ^{O}C for 2 h, another exposure to UV radiation for 2 h, and final gamma irradiation at the dose of 250 krad; **dark green** exposure to UV for 2 h, followed by a gamma irradiation at the dose of 250 krad, a temperature stress at 140 ^{O}C for 2 h, a new exposure to UV radiation for 2 h; a new gamma irradiation at the dose of 250 krad, and a final exposure to UV radiation for 2 h; **violet**: exposure to UV radiation for 2 h, followed by a gamma irradiation at the dose of 250 krad, a temperature stress at 140 ^{O}C for 2 h, a new exposure to UV radiation for 2 h, a new gamma irradiation at the dose of 250 krad, a new exposure to UV radiation for 2 h, and a final thermal stress at 140 ^{O}C for 4 h.

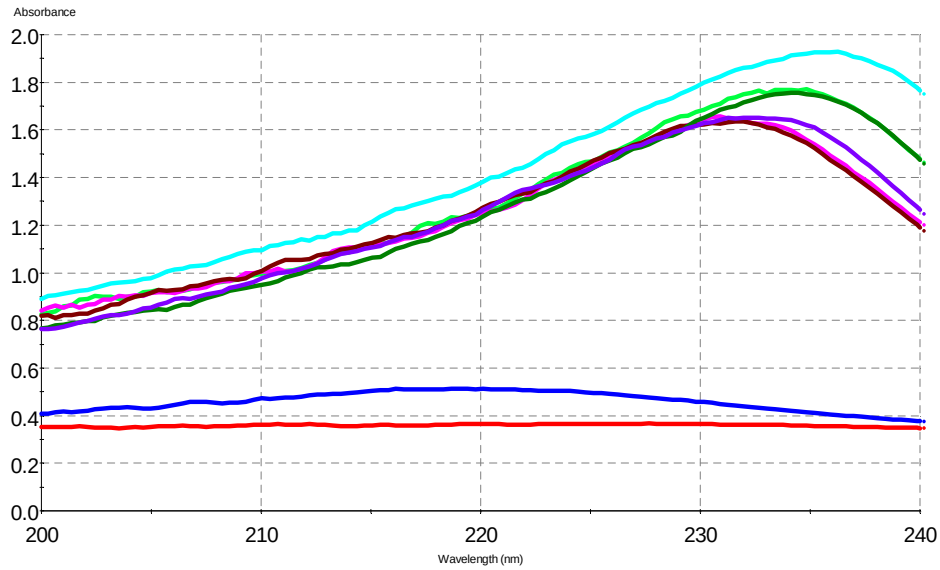

Figure 10. The spectral interval 200 nm – 240 nm.

In the case we consider the base-line from the spectrum graphs as the absorption corresponding to the non-irradiated optical fibers (a value of 0.7 units in a logarithmic scale), one can evaluate radiation-induced changes. For such a situation, our investigations indicate:

- the wavelength corresponding to the peak absorption is at about 220 nm;
- the UV induced absorption sees to saturate (i.e. a 2 h UV exposure induces an absorption peak of 0.9 units, a 6 h exposure one of 1.05 units, while an exposure of 10 h produces a peak of 1.08 units);
- temperature stress applied after UV exposure reduces the optical absorption in a limited range (about 0.4 - 0.6 units);

- the peak for gamma induced optical absorption is located between 230 nm and 235 nm, depending on the gamma total dose and the temperature stress applied;
- in the case of pure gamma irradiation (no UV exposure) a temperature stress reduces the absorption peak by 0.3 unit;
- any temperature treatment following a gamma irradiation produces a decrease of the optical absorption, but the radiation effect can not be reduced completely;
- it seems gamma irradiation is the dominant effect with respect to the UV-induced optical absorption;
- it is difficult to compare the recovering phenomena produced by heating after UV exposure steps and gamma irradiation steps as far as the changes are comparable with the accuracy of the readings (limited by the losses in connectors).

In the next year, the investigations will focus on the effect of gamma-ray and neutron irradiation on UV solarization resistant optical fibers, by studying the radiation induced modifications in their optical absorption in the UV spectral range.

Publications:

[1] **Sporea D., "***Investigation of the properties of optical fibers (in the UV spectral region) and optoelectronic components operating in radiation fields of fusion installations",* Association EURATOM MEC, Romania, Annual Report 2001, UT-1, 20.

[2] **Sporea D**., "*Study of uncertainties in laser diodes parameters evaluation"*, paper to be submitted for publication.

[3] **Sporea D**., "4th Meeting of the ITPA Topical Group on Diagnostics" Padova, Italy, 2003.

[4] **Sporea D**., "*Gamma-ray induced absorption in optical fibers used for plasma diagnostics",* 2003 IEEE International Conference on Plasma Science, Jeju, Korea, June, 2003..

[5] **Sporea D**. **and Florean A.**, "*Investigations on the degradation of visible laser diodes under gamma-ray irradiation"*, Fusion Engineering and Design, 66-68, (2003), 877.